


Applications of Voltage-Based Power Control using Online Load Sensitivity Calculation

Maëva Courcelle

Institute of Technical Physics (ITEP)

Karlsruhe Institute of Technology (KIT)

Karlsruhe, Germany


 0000-0002-7310-6338

Qiucen Tao

Institute of Technical Physics (ITEP)

Karlsruhe Institute of Technology (KIT)

Karlsruhe, Germany


 0000-0003-2115-3885

Giovanni De Carne

Institute of Technical Physics (ITEP)

Karlsruhe Institute of Technology (KIT)

Karlsruhe, Germany

 0000-0002-3700-2902

Abstract—The increasing integration of renewable energy resources prompts a reevaluation of the controllability of power generation within the electrical grid. In response, research explores demand-side management options to increase flexibility by enhancing control on the load side. The voltage-based load management method enables control of the power consumption from the utility side through power electronic-based interfaces, such as the Solid State Transformers. The power is regulated by adjusting the voltage magnitude using the correlation between the load power and voltage, also known as load sensitivity to voltage. This method requires accurate and updated values of the load sensitivity. However, previous works have applied a constant voltage sensitivity value, assumed to be known, without regard to the time-varying load. This study presents an experimentally validated power control of a household load induced by a change in voltage amplitude, where the voltage set-point calculation is based on the real-time evaluation and updated value of the load sensitivity.

Index Terms—Load Sensitivity, Demand-Side Management, Voltage Control, Solid-State Transformer.

I. INTRODUCTION

While the dynamics and control of power generation are evolving, the concept of demand-side management offers compensatory flexibility by directly influencing the power consumption of the loads. In [1], [2], overviews of direct or indirect approaches to load management are provided. The latter suggests the customers shift or reduce their consumption based on factors like market price, or incentives [3], [4]. However, the variation in power consumption depends highly on the customers' decisions which are not under control. A direct load control, instead, provides power flexibility through for instance interruptible/curtailment programs, or by communicating directly with single appliances. These methods face obvious obstacles in terms of customer acceptance and dealing with the huge amount of data and communication [5]–[8].

These concerns are overcome with the voltage-led power control, where the load consumption is affected by a change in voltage amplitude conducted by the utility side [9]–[12]. It uses a similar concept as the established technology

Conservative Voltage Reduction (CVR), which is widely applied in substations in US [13]. Assuming that part of the connected loads are sensitive to voltage, the total power consumption will be impacted by the change in voltage amplitude. The concept has been extended to a smaller granularity using power-electronic devices, particularly, Solid State Transformers (SST) [11], [14]. Although there is currently no commercial product, several industrial projects are investigating the feasibility and business case as the technology is promising and will be integrated into the distribution grid in the coming years. Acting as grid-forming units, SST can dynamically modulate the voltage parameters, namely amplitude and frequency, by means of a voltage control loop [15]–[18]. The control of SST can be based on load sensitivity, which describes the percentage of power change resulting from a variation of 1% of voltage amplitude change [19], [20]. The load sensitivity varies over time and depends on the current state of the grid, which was usually ignored in previous works [21]–[23]. To keep the voltage sensitivity value updated, an online calculation can be applied [24].

However, previous works did not validate experimentally the load sensitivity calculation in realistic conditions, where the calculation has been carried on in real-time. This study explores the concept of voltage-led power control using triggered online load sensitivity calculation. The work demonstrates this control in a Power Hardware-In-the-Loop (PHIL) environment with real-time calculation of the load sensitivity [25]–[27].

The rest of the paper is structured as follows. In Section II, the load sensitivity is defined, and the calculation method is explained. Section III focuses on the PHIL experimental implementation and results. Finally, conclusions are drawn in Section IV.

II. VOLTAGE SENSITIVITY AND CALCULATION METHOD

This section aims to mathematically define the load sensitivity to voltage and introduce its calculation method.

This work has been supported by the Helmholtz Association under the program "Energy System Design" and under the Helmholtz Young Investigator Group "Hybrid Networks" (VH-NG-1613).

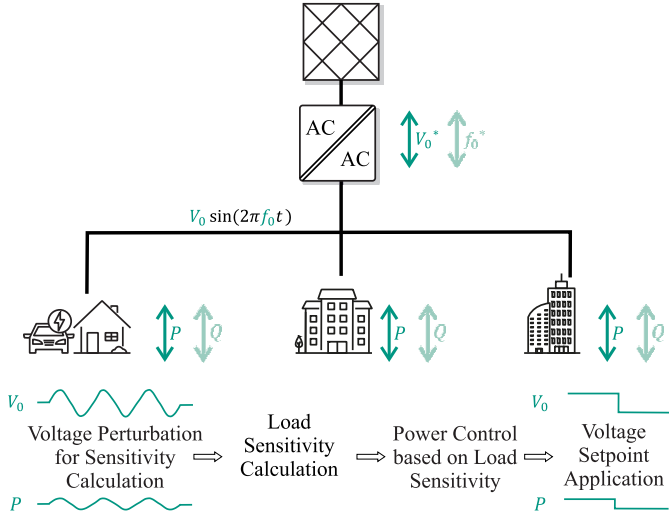


Fig. 1: Concept of voltage-based power control for demand-side management, using load sensitivity.

A. Definitions

Equations (1) and (2) define the load active (resp. reactive) power sensitivity to voltage amplitude change:

$$K_{pv} = \frac{\Delta P/P_0}{\Delta V/V_0} \quad (1)$$

$$K_{qv} = \frac{\Delta Q/Q_0}{\Delta V/V_0} \quad (2)$$

where K_{pv} and K_{qv} are the load sensitivity to voltage, V is the voltage amplitude, P (resp. Q) is the active (resp. reactive) power, V_0 is the rated voltage, and P_0 (resp. Q_0) is the rated active (resp. reactive) power.

Equations (1) and (2) can be seen as linearizations of the exponential load model, expressed in equations (3) and (4).

$$P = P_0 \cdot \left(\frac{V}{V_0}\right)^{K_{pv}} \quad (3)$$

$$Q = Q_0 \cdot \left(\frac{V}{V_0}\right)^{K_{qv}} \quad (4)$$

where the exponent K_{pv} (resp. K_{qv}) is exactly the load sensitivity to voltage.

In practice, the load sensitivity calculation is based on a simultaneous variation in voltage amplitude and power, where at least two values of the power (resp. voltage) are measured and injected in (1) [19]. This leads to the following load sensitivity calculation:

$$K_{pv} = \frac{(P_2 - P_1)/P_1}{(V_2 - V_1)/V_1} \quad (5)$$

with (V_1, P_1) the measurements of voltage and power at $t = t_1$, and (V_2, P_2) the measurements at $t = t_2$, where $t_2 = t_1 + t_s$ and t_s is the time step between two measurements. The relation is obviously also valid for reactive power.

B. Perturbation-Based Load Sensitivity Identification

The load sensitivity calculation, as stated in subsection II-A, requires voltage and power measurements of a simultaneous change in voltage amplitude and power of the connected load. This can be caused by natural fluctuations of the voltage amplitude or artificially generated voltage variations, that are fully controlled. As stressed in Fig. 1, this work is based on the assumption that loads are interfaced to the grid with a power electronic converter, acting as a grid-forming converter for the low-voltage side. Therefore, the voltage is controlled and a short (~ 1 s) perturbation in the voltage amplitude can be applied. During this created perturbation, the calculation of the load sensitivity, defined in (5), can be implemented.

Fig. 1 shows the use of a perturbation for load sensitivity calculation in the voltage-based power control process. [24] shows the accuracy of the calculation, injecting measurements of a controlled perturbation in (5) for the calculation of the load sensitivity.

C. Voltage-based Power Control

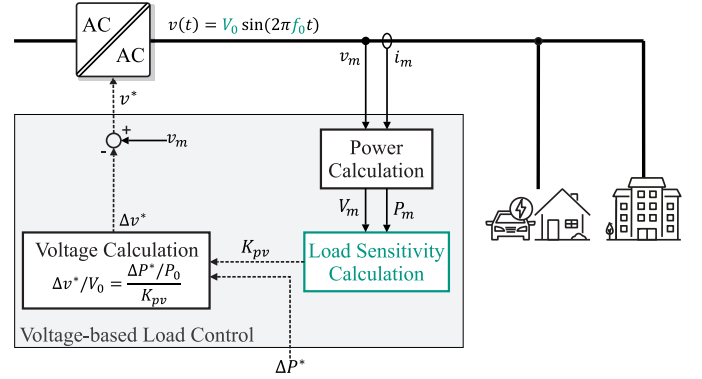


Fig. 2: Overview of voltage-based power control by means of SST, using online calculated load sensitivity.

To keep the power balance in the grid, we assume that a power variation ΔP^* is required. ΔP^* is for example the difference between the generated power P_{gen} and the actual power consumption P_{load} . The voltage-based power control aims to apply the appropriate voltage drop ΔV^* , leading to the requested power drop. The fitting voltage drop can easily be calculated with the knowledge of the actual load sensitivity [15].

Indeed, based on the load sensitivity definition of (1), the voltage variation which should be applied to compensate the excess of consumed power is simply:

$$\Delta V^* = \frac{V_0}{K_{pv} \cdot P_0} \cdot \Delta P^* \quad (6)$$

where K_{pv} is the calculated load sensitivity to voltage, ΔP^* is the power variation request, ΔV^* is the voltage variation set-point to be applied to the SST, with $\Delta V^* = V^* - V_0$, $\Delta P^* = P^* - P_0$, and V_0 and P_0 are the normalization points, namely, the measurement state before the perturbation used for the load sensitivity calculation.

The use of load sensitivity calculation for voltage-based power control by means of SST is summarized in Fig. 2.

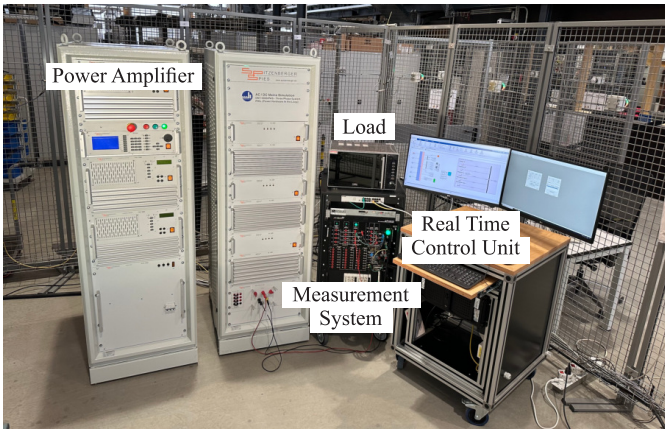
III. EXPERIMENTAL VALIDATION OF VOLTAGE-BASED POWER CONTROL

This section details the Power Hardware-In-the-Loop (PHIL) setup used for the voltage-based power control, where a microwave oven is used as a showcase.

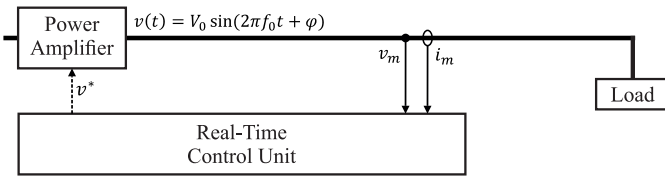
A. Control Implementation

This section focuses on the implementation of the voltage-based power control introduced in subsection II-C.

1) *Experimental setup*: A real-time control unit generates the voltage set-point, which is subsequently sent to the power amplifier. The power supplied by the amplifier energizes the load, in this case, a microwave, as shown in Fig. 3. To monitor and regulate this process, voltage and current sensors are connected to the system, where measurements are received by the analog inputs of the real-time simulator. Exploiting the acquired measurements, the control unit calculates the voltage amplitude and powers (active and reactive). The load sensitivity is determined in real-time based on the voltage amplitude and power metrics. The voltage control based on the load sensitivity is then implemented in the real-time control unit.



(a)



(b)

Fig. 3: (a) Experimental setup for the voltage-based power control, using a microwave as a showcase. (b) Schematic representation of the setup.

2) *Load sensitivity calculation*: Fig. 4 displays the scenario used for the experiment. The first graph shows the power reference P^*/P_0 , while the second graph highlights the time

windows when the perturbations used for load sensitivity calculation are triggered.

The perturbations in voltage amplitude (V_{RMS}), triggered at $t = 20$ s and at $t = 120$ s, are sinusoidal waves having the amplitude of 1% of V_0 . Each perturbation lasts 1.5 periods of the 0.8 Hz sinusoidal wave. During the perturbations, the load sensitivity is calculated based on voltage and power measurements. The load sensitivity is calculated during the entire perturbation window, but for accuracy purposes, only the load sensitivity values of one full perturbation period (center of the 1.5-period sinus perturbation) are considered. By doing so, the impact of the inefficiency of the Hampel filter at the start and the end of the data set is reduced. After filtering the load sensitivity values and selecting the proper time window, the average is calculated, delivering the actual load sensitivity value. This final load sensitivity is updated after each perturbation event and used for the control.

Furthermore, the rated voltage V_0 and rated power P_0 are required for the control. The voltage amplitude and power are continuously averaged over a 3-second time window. As soon as a new perturbation is triggered, these 3-second average of voltage and power are assigned to V_0 and P_0 for an update. The array $\{V_0; P_0; K_{pv}\}$ is kept constant until the next update and is used for the following voltage control.

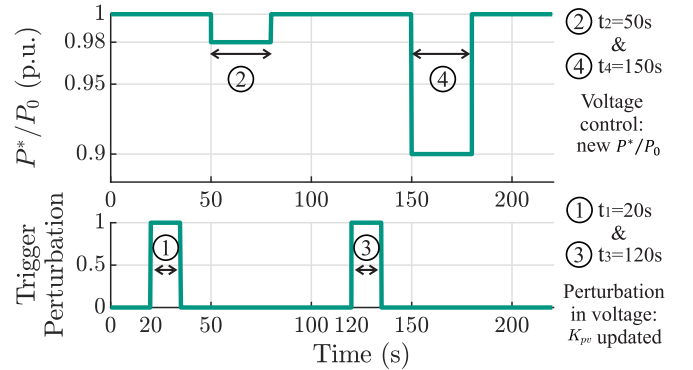


Fig. 4: Experimental scenario showing the power request P^*/P_0 (where a control is requested when $P^* \neq P_0$), and the perturbation trigger.

3) *Voltage control*: The voltage control relies not only on the actual load sensitivity but also on the array $\{V_0; P_0; K_{pv}\}$. (6) depicts the voltage control as a simple proportional control, where the voltage set-point calculation V^* can be expressed as follows:

$$V^* = V_0 \cdot \left(1 - \frac{1}{K_{pv}} \cdot \left(1 - \frac{P^*}{P_0}\right)\right) \quad (7)$$

where K_{pv} is the calculated load sensitivity to voltage, P^*/P_0 is the power variation request, V^* is the voltage set-point to be applied, and V_0 and P_0 are the normalization points, namely, the measurement state before the perturbation.

To stay in the electrical grid norms and not damage the connected load, upper and lower thresholds are set for the

voltage drop:

$$\Delta V_{max} = \pm 5\% \cdot V_{nom} \quad (8)$$

with the nominal voltage $V_{nom} = 230$ V.

This threshold is for example reached when the load sensitivity K_{pv} regarding the rated power P_0 does not allow to reach the desired power P^* for a voltage drop within $\pm 5\%$.

B. Results

The outcomes of the voltage-based control, as outlined in the previous section, are visualized in Fig. 5. The voltage amplitude and the power of the load have been recorded, and the related updated load sensitivity K_{pv} is plotted in the third graph. The experiment, including the load sensitivity calculation, has been repeated eleven independent times. The grey area highlights the variability of the load across these tests. The red curves depict the average values derived from this set of experiments.

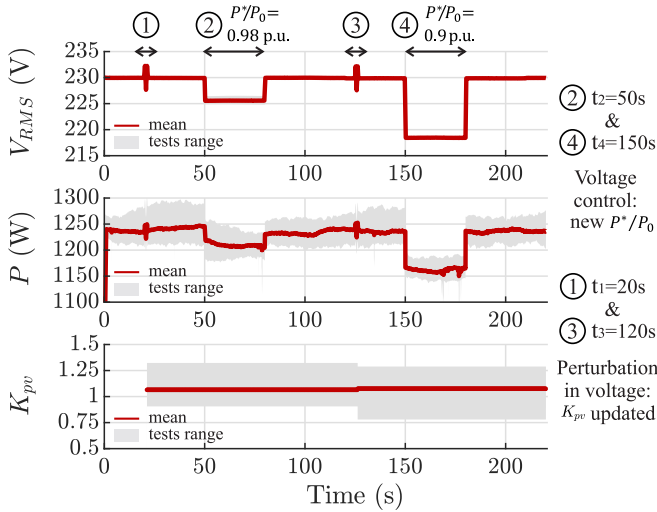


Fig. 5: Voltage-based control of the power of a microwave.

1) *Load sensitivity update:* Following the scenario of Fig. 4, the load sensitivity is calculated during the voltage amplitude perturbations occurring at $t_1 = 20$ s and $t_3 = 120$ s, and is updated with the mean of the calculation set. On average, considering the eleven measurements, the sensitivity of the microwave power to voltage was equal to $K_{pv} = 1.06$ after the first update and $K_{pv} = 1.07$ after the second update.

2) *Voltage Control at $t_2 = 50$ s:* At t_2 , voltage control is required to respond to the request of a 2% decrease in power. For this first control, on average the following array $\{V_0 = 230$ V; $P_0 = 1235$ W; $K_{pv} = 1.06\}$ has been recorded. As a consequence, the voltage set-point to be applied is $V^* = 225.6$ V in average, which corresponds to $\Delta V/V_0 = 1.91\%$.

The initial objective was to achieve a reduction of 2% in power, with respect to the rated power P_0 . However, actual loads often exhibit variable power, rendering the previously considered array potentially invalid for control purposes at a later time. In this case, the control is applied 30 s after the array

calculation. The real power drop (expressed in percentage) between the power levels before and after the applied voltage reduction is visualized in Fig. 6. Both power level values are 1 second-average of the measured power before and after the drop. The first graph shows the real power drop for each independent eleven measurements in green, where the mean drop is highlighted in red. The dashed red line represents the target drop of 2%.

The drop deviation from the reference E_r is represented in the second graph. E_r depicts the difference between the target power P^* and the actual power P_{actual} based on the real power drop:

$$E_r = \frac{P_{actual} - P^*}{P^*} \quad (9)$$

where $P^* = \Delta P^* \cdot P_0$ and $P_{actual} = \Delta P \cdot P_0$, and ΔP is the real measured power drop.

From Fig. 6 it is observable that the disparity between the anticipated power reduction of 2% and the observed drop is small, with an average error $E_r = 0.18\%$ (red marker).

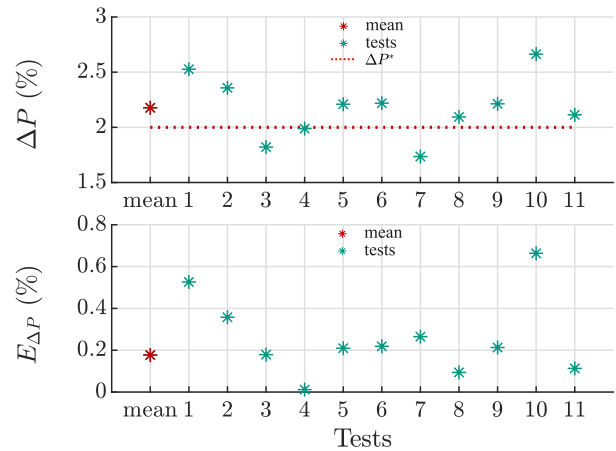


Fig. 6: Error of the voltage-based power control.

3) *Voltage Control at $t_4 = 150$ s:* For this second calculation, 10% of power drop is requested. The second array calculation occurring at t_3 gives the following results: $\{V_0 = 229.8$ V; $P_0 = 1240$ W; $K_{pv} = 1.07\}$. With this combination, ΔV^* should reach 9.4%, which is much more than the limit of 5%. Thus, the maximum voltage drop ΔV_{max} is applied, leading to a power drop of $\Delta P/P_0 = \Delta V/V_0 \cdot K_{pv} = 5.4\%$. This power reduction is well noticeable in Fig. 5, where at t_4 the power fall from $P_0 = 1240$ W to $P_{-5.4\%} = 1178$ W $\pm E_r$.

4) *Summary:* This section has demonstrated the effectiveness of a straightforward voltage-based power control, employing load sensitivity. In this showcase, a microwave was connected to the controllable voltage supply.

The scope of this work can be broadened to more complex control scenarios, wherein the objective extends beyond merely reducing power but also includes the management of the absolute power value. Incorporating a set of loads would also better represent the real environment of an SST, where

the load sensitivity will be updated depending on the system's behavior.

IV. CONCLUSION

In this work, the control of the power of a load was induced by a change in voltage amplitude, where the voltage set-point calculation was based on a real-time evaluation of the load sensitivity. The effectiveness of the voltage-based power control was demonstrated in a PHIL environment, showcasing the precise power consumption reduction of a typical load. This reduction was aligned to predefined requirements with an average error of less than 0.2%.

In an electrical grid with integrated actuators like a solid-state transformer, this voltage-based power control increases the flexibility by providing ancillary services like peak shaving without disconnecting the loads, or control reserve by minimizing the use of the load following power plants.

REFERENCES

- [1] K. Kostková, L. Omelina, P. Kycina, and P. Jamrich, "An introduction to load management," *Electric Power Systems Research*, vol. 95, pp. 184–191, 2013. [Online]. Available: <https://www.sciencedirect.com/science/article/pii/S037877961200288X>
- [2] E. Sarker, P. Halder, M. Seyedmahmoudian, E. Jamei, B. Horan, S. Mekhilef, and A. Stojcevski, "Progress on the demand side management in smart grid and optimization approaches," *International Journal of Energy Research*, vol. 45, no. 1, p. 36–64, 2020.
- [3] L. Scharnhorst, T. Sandmeier, A. Ardone, and W. Fichtner, "The impact of economic and non-economic incentives to induce residential demand response—findings from a living lab experiment," *Energies*, vol. 14, no. 8, 2021. [Online]. Available: <https://www.mdpi.com/1996-1073/14/8/2036>
- [4] K. Herter, "Residential implementation of critical-peak pricing of electricity," *Energy Policy*, vol. 35, no. 4, pp. 2121–2130, 2007. [Online]. Available: <https://www.sciencedirect.com/science/article/pii/S0301421506002783>
- [5] G. Strbac, "Demand side management: Benefits and challenges," *Energy Policy*, vol. 36, no. 12, pp. 4419–4426, 2008, foresight Sustainable Energy Management and the Built Environment Project. [Online]. Available: <https://www.sciencedirect.com/science/article/pii/S0301421508004606>
- [6] Y. Yan, Y. Qian, H. Sharif, and D. Tipper, "A survey on smart grid communication infrastructures: Motivations, requirements and challenges," *IEEE Communications Surveys Tutorials*, vol. 15, no. 1, pp. 5–20, 2013.
- [7] A. Paverd, A. Martin, and I. Brown, "Security and privacy in smart grid demand response systems," in *Smart Grid Security*, J. Cuellar, Ed. Cham: Springer International Publishing, 2014, pp. 1–15.
- [8] Y. Gong, Y. Cai, Y. Guo, and Y. Fang, "A privacy-preserving scheme for incentive-based demand response in the smart grid," *IEEE Transactions on Smart Grid*, vol. 7, no. 3, pp. 1304–1313, 2016.
- [9] A. Ballanti, L. N. Ochoa, K. Bailey, and S. Cox, "Unlocking new sources of flexibility: Class: The world's largest voltage-led load-management project," *IEEE Power and Energy Magazine*, vol. 15, no. 3, pp. 52–63, 2017.
- [10] A. Ballanti and L. F. Ochoa, "Voltage-led load management in whole distribution networks," *IEEE Transactions on Power Systems*, vol. 33, no. 2, pp. 1544–1554, 2018.
- [11] G. De Carne, G. Buticchi, M. Liserre, and C. Vournas, "Load control using sensitivity identification by means of smart transformer," *IEEE Transactions on Smart Grid*, vol. 9, no. 4, pp. 2606–2615, 2016.
- [12] A. Gorjian, M. Eskandari, and M. H. Moradi, "Conservation voltage reduction in modern power systems: Applications, implementation, quantification, and ai-assisted techniques," *Energies*, vol. 16, no. 5, 2023. [Online]. Available: <https://www.mdpi.com/1996-1073/16/5/2502>
- [13] Z. Wang and J. Wang, "Review on implementation and assessment of conservation voltage reduction," *IEEE Transactions on Power Systems*, vol. 29, no. 3, pp. 1306–1315, 2014.
- [14] M. Liserre, G. Buticchi, M. Andresen, G. De Carne, L. F. Costa, and Z.-X. Zou, "The smart transformer: Impact on the electric grid and technology challenges," *IEEE Industrial Electronics Magazine*, vol. 10, no. 2, pp. 46–58, 2016.
- [15] G. De Carne, G. Buticchi, M. Liserre, and C. Vournas, "Load control using sensitivity identification by means of smart transformer," *IEEE Transactions on Smart Grid*, vol. 9, no. 4, pp. 2606–2615, 2018.
- [16] Q. Tao, J. Geis-Schroer, F. Wald, M. Courcelle, M. Langwasser, T. Leibfried, M. Liserre, and G. De Carne, "The potential of frequency-based power control in distribution grids," in *2022 IEEE 13th International Symposium on Power Electronics for Distributed Generation Systems (PEDG)*, 2022, pp. 1–6.
- [17] F. Wald, Q. Tao, and G. D. Carne, "Virtual synchronous machine control for asynchronous grid connections," *IEEE Transactions on Power Delivery*, pp. 1–10, 2023.
- [18] F. Wald and G. De Carne, "Adaptive virtual synchronous machine control for asynchronous grid connections," in *2023 11th International Conference on Power Electronics and ECCE Asia (ICPE 2023 - ECCE Asia)*, 2023, pp. 991–996.
- [19] G. De Carne, M. Liserre, and C. Vournas, "On-line load sensitivity identification in lv distribution grids," *IEEE Transactions on Power Systems*, vol. 32, no. 2, pp. 1570–1571, 2017.
- [20] G. De Carne, S. Bruno, M. Liserre, and M. La Scala, "Distributed online load sensitivity identification by smart transformer and industrial metering," *IEEE Transactions on Industry Applications*, vol. 55, no. 6, pp. 7328–7337, 2019.
- [21] L. Hajagos and B. Danai, "Laboratory measurements and models of modern loads and their effect on voltage stability studies," *IEEE Transactions on Power Systems*, vol. 13, no. 2, pp. 584–592, 1998.
- [22] A. Bokhari, A. Alkan, R. Dogan, M. Diaz-Aguiló, F. de León, D. Czarkowski, Z. Zabar, L. Birenbaum, A. Noel, and R. E. Usef, "Experimental determination of the zip coefficients for modern residential, commercial, and industrial loads," *IEEE Transactions on Power Delivery*, vol. 29, no. 3, pp. 1372–1381, 2014.
- [23] A. Arif, Z. Wang, J. Wang, B. Mather, H. Bashualdo, and D. Zhao, "Load modeling—a review," *IEEE Transactions on Smart Grid*, vol. 9, no. 6, pp. 5986–5999, 2018.
- [24] M. Courcelle, Q. Tao, J. Geis-Schroer, S. Bruno, T. Leibfried, and G. De Carne, "Methods comparison for load sensitivity identification," in *2023 IEEE Belgrade PowerTech*, 2023, pp. 1–6.
- [25] G. F. Lauss, M. O. Faruque, K. Schoder, C. Dufour, A. Viehweider, and J. Langston, "Characteristics and design of power hardware-in-the-loop simulations for electrical power systems," *IEEE Transactions on Industrial Electronics*, vol. 63, no. 1, pp. 406–417, 2016.
- [26] A. Benigni, T. Strasser, G. De Carne, M. Liserre, M. Cupelli, and A. Monti, "Real-time simulation-based testing of modern energy systems: A review and discussion," *IEEE Industrial Electronics Magazine*, vol. 14, no. 2, pp. 28–39, 2020.
- [27] G. De Carne, G. Lauss, M. H. Syed, A. Monti, A. Benigni, S. Karrari, P. Kotsampopoulos, and M. O. Faruque, "On modeling depths of power electronic circuits for real-time simulation – a comparative analysis for power systems," *IEEE Open Access Journal of Power and Energy*, vol. 9, pp. 76–87, 2022.